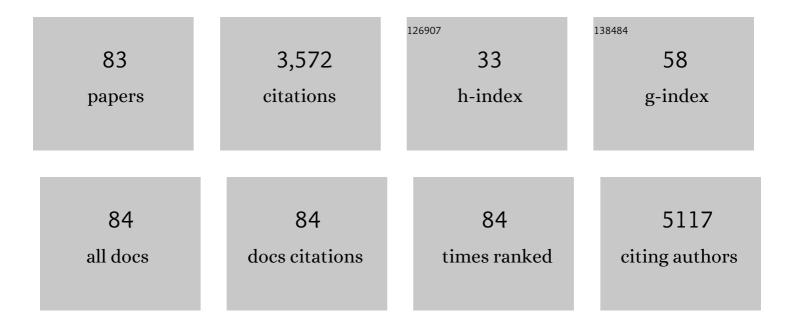
## **Thomas Feurer**

List of Publications by Year in descending order

Source: https://exaly.com/author-pdf/2529173/publications.pdf Version: 2024-02-01



THOMAS FELIDED

#	Article	IF	CITATIONS
1	How band tail recombination influences the openâ€eircuit voltage of solar cells. Progress in Photovoltaics: Research and Applications, 2022, 30, 702-712.	8.1	35
2	CNT-based bifacial perovskite solar cells toward highly efficient 4-terminal tandem photovoltaics. Energy and Environmental Science, 2022, 15, 1536-1544.	30.8	39
3	Inverse-Designed Narrowband THz Radiator for Ultrarelativistic Electrons. ACS Photonics, 2022, 9, 1143-1149.	6.6	5
4	Optically Controlled Electron Transfer in a Re <sup>I</sup> Complex. Chemistry - A European Journal, 2021, 27, 5399-5403.	3.3	6
5	Ultrashort pulse formation from a thulium-doped fiber laser: Self-characterization and mapping. Optics Communications, 2021, 486, 126747.	2.1	5
6	3D-printed THz wave- and phaseplates. Optics Express, 2021, 29, 27160.	3.4	16
7	Terahertz Selective Emission Enhancement from a Metasurface-Coupled Photoconductive Emitter in Quasi-Near-Field Zone. Plasmonics, 2020, 15, 263-269.	3.4	3
8	Graphene Metamaterials for Intense, Tunable, and Compact Extreme Ultraviolet and Xâ€Ray Sources. Advanced Science, 2020, 7, 1901609.	11.2	21
9	Towards jitter-free ultrafast electron diffraction technology. Nature Photonics, 2020, 14, 245-249.	31.4	55
10	Revealing the perovskite formation kinetics during chemical vapour deposition. Journal of Materials Chemistry A, 2020, 8, 21973-21982.	10.3	24
11	Nearâ€Infraredâ€Transparent Perovskite Solar Cells and Perovskiteâ€Based Tandem Photovoltaics. Small Methods, 2020, 4, 2000395.	8.6	63
12	DNA-organized artificial LHCs – testing the limits of chromophore segmentation. Organic and Biomolecular Chemistry, 2020, 18, 6818-6822.	2.8	7
13	Anti-Kasha Conformational Photoisomerization of a Heteroleptic Dithiolene Metal Complex Revealed by Ultrafast Spectroscopy. Journal of Physical Chemistry A, 2020, 124, 10687-10693.	2.5	8
14	High-Mobility In <sub>2</sub> O <sub>3</sub> :H Electrodes for Four-Terminal Perovskite/CuInSe <sub>2</sub> Tandem Solar Cells. ACS Nano, 2020, 14, 7502-7512.	14.6	54
15	Photocycle of Excitons in Nitrogen-Rich Carbon Nanodots: Implications for Photocatalysis and Photovoltaics. ACS Applied Nano Materials, 2020, 3, 6925-6934.	5.0	11
16	ALD-ZnMgO and absorber surface modifications to substitute CdS buffer layers in co-evaporated CIGSe solar cells. EPJ Photovoltaics, 2020, 11, 12.	1.6	6
17	Temporal fine structure of all-normal dispersion fiber supercontinuum pulses caused by non-ideal pump pulse shapes. Optics Express, 2020, 28, 16579.	3.4	17
18	Extending time-domain ptychography to generalized phase-only transfer functions. Optics Letters, 2020, 45, 300.	3.3	9

#	Article	IF	CITATIONS
19	High-resolution phase-sensitive sum frequency generation spectroscopy by time-domain ptychography. Optics Letters, 2020, 45, 6082-6085.	3.3	0
20	Efficiency Improvement of Nearâ€Stoichiometric CuInSe <sub>2</sub> Solar Cells for Application in Tandem Devices. Advanced Energy Materials, 2019, 9, 1901428.	19.5	69
21	DNAâ€Organized Lightâ€Harvesting Antennae: Energy Transfer in Polyaromatic Stacks Proceeds through Interposed Nucleobase Pairs. Helvetica Chimica Acta, 2019, 102, e1900148.	1.6	4
22	Advanced Alkali Treatments for Highâ€Efficiency Cu(In,Ga)Se <sub>2</sub> Solar Cells on Flexible Substrates. Advanced Energy Materials, 2019, 9, 1900408.	19.5	175
23	Tunable Lifetimes of Intramolecular Charge-Separated States in Molecular Donor–Acceptor Dyads. Journal of Physical Chemistry C, 2019, 123, 8500-8511.	3.1	9
24	Bulk and surface recombination properties in thin film semiconductors with different surface treatments from time-resolved photoluminescence measurements. Scientific Reports, 2019, 9, 5385.	3.3	65
25	Bandgap of thin film solar cell absorbers: A comparison of various determination methods. Thin Solid Films, 2019, 669, 482-486.	1.8	56
26	RbF post deposition treatment for narrow bandgap Cu(In,Ga)Se2 solar cells. Thin Solid Films, 2019, 670, 34-40.	1.8	33
27	Ultra low-noise coherent supercontinuum amplification and compression below 100 fs in an all-fiber polarization-maintaining thulium fiber amplifier. Optics Express, 2019, 27, 35041.	3.4	34
28	Dipole Moment and Polarizability of Tunable Intramolecular Charge Transfer States in Heterocyclic Ï€-Conjugated Molecular Dyads Determined by Computational and Stark Spectroscopic Study. Journal of Physical Chemistry C, 2018, 122, 9346-9355.	3.1	13
29	Cu(In,Ca)Se2 solar cells on low cost mild steel substrates. Solar Energy, 2018, 175, 25-30.	6.1	35
30	Compositionally Graded Absorber for Efficient and Stable Nearâ€Infraredâ€Transparent Perovskite Solar Cells. Advanced Science, 2018, 5, 1700675.	11.2	65
31	Single-graded CIGS with narrow bandgap for tandem solar cells. Science and Technology of Advanced Materials, 2018, 19, 263-270.	6.1	51
32	Tailored lead iodide growth for efficient flexible perovskite solar cells and thin-film tandem devices. NPG Asia Materials, 2018, 10, 1076-1085.	7.9	35
33	Attoclock Ptychography. Applied Sciences (Switzerland), 2018, 8, 1039.	2.5	4
34	Refractive indices of layers and optical simulations of Cu(In,Ga)Se <sub>2</sub> solar cells. Science and Technology of Advanced Materials, 2018, 19, 396-410.	6.1	46
35	Solutionâ€Processed Lowâ€Bandgap CuIn(S,Se) <sub>2</sub> Absorbers for Highâ€Efficiency Singleâ€Junction and Monolithic Chalcopyriteâ€Perovskite Tandem Solar Cells. Advanced Energy Materials, 2018, 8, 1801254.	19.5	56
36	Terahertz ptychography. Optics Letters, 2018, 43, 543.	3.3	57

#	Article	IF	CITATIONS
37	Disentangling size effects and spectral inhomogeneity in carbon nanodots by ultrafast dynamical hole-burning. Nanoscale, 2018, 10, 15317-15323.	5.6	33
38	Novel back contact reflector for high efficiency and doubleâ€graded Cu(In,Ga)Se <sub>2</sub> thinâ€film solar cells. Progress in Photovoltaics: Research and Applications, 2018, 26, 894-900.	8.1	14
39	Chromium nitride as a stable cathode current collector for all-solid-state thin film Li-ion batteries. RSC Advances, 2017, 7, 26960-26967.	3.6	11
40	Flexible NIR-transparent perovskite solar cells for all-thin-film tandem photovoltaic devices. Journal of Materials Chemistry A, 2017, 5, 13639-13647.	10.3	68
41	Monolithic CIGS–Perovskite Tandem Cell for Optimal Light Harvesting without Current Matching. ACS Photonics, 2017, 4, 861-867.	6.6	27
42	Impact of compositional grading and overall Cu deficiency on the near-infrared response in Cu(In,) Tj ETQq0 0 0	rgBT /Over 8.1	loçk 10 Tf 50
43	High-efficiency inverted semi-transparent planar perovskite solar cells in substrate configuration. Nature Energy, 2017, 2, .	39.5	247
44	Precise Se-flux control and its effect on Cu(In,Ga)Se 2 absorber layer deposited at low substrate temperature by multi stage co-evaporation. Thin Solid Films, 2017, 633, 18-22.	1.8	12
45	Progress in thin film CIGS photovoltaics – Research and development, manufacturing, and applications. Progress in Photovoltaics: Research and Applications, 2017, 25, 645-667.	8.1	248
46	Self-photopumped x-ray lasers from elements in the Ne-like and Ni-like ionization state. Optics Communications, 2017, 382, 288-293.	2.1	5
47	Improved retrieval of complex supercontinuum pulses from XFROG traces using a ptychographic algorithm. Optics Letters, 2016, 41, 4903.	3.3	25
48	Surface Passivation for Reliable Measurement of Bulk Electronic Properties of Heterojunction Devices. Small, 2016, 12, 5339-5346.	10.0	17
49	THz near-field enhancement by means of isolated dipolar antennas: the effect of finite sample size. Optics Express, 2016, 24, 4552.	3.4	14
50	Controlled growth of PbI <sub>2</sub> nanoplates for rapid preparation of CH <sub>3</sub> NH <sub>3</sub> PbI <sub>3</sub> in planar perovskite solar cells. Physica Status Solidi (A) Applications and Materials Science, 2015, 212, 2708-2717.	1.8	63
51	High-Efficiency Polycrystalline Thin Film Tandem Solar Cells. Journal of Physical Chemistry Letters, 2015, 6, 2676-2681.	4.6	166
52	Solvation-Driven Charge Transfer and Localization in Metal Complexes. Accounts of Chemical Research, 2015, 48, 1432-1440.	15.6	39
53	Pulse-shaping assisted multidimensional coherent electronic spectroscopy. Journal of Chemical Physics, 2015, 142, 212451.	3.0	7
54	Low-temperature-processed efficient semi-transparent planar perovskite solar cells for bifacial and tandem applications. Nature Communications, 2015, 6, 8932.	12.8	398

#	Article	IF	CITATIONS
55	THz generation by optical rectification of near-infrared laser pulses in the organic nonlinear optical crystal HMQ-TMS. Optical Materials Express, 2014, 4, 1586.	3.0	33
56	Skirting terahertz waves in a photo-excited nanoslit structure. Applied Physics Letters, 2014, 104, .	3.3	10
57	Comparative theoretical analysis of continuous wave laser cutting of metals at 1 and 10Âμm wavelength. Applied Physics A: Materials Science and Processing, 2014, 116, 1353-1364.	2.3	8
58	Optimization-Based Terahertz Imaging. IEEE Transactions on Terahertz Science and Technology, 2012, 2, 493-503.	3.1	5
59	High Aspect Ratio Plasmonic Nanostructures for Sensing Applications. ACS Nano, 2011, 5, 6374-6382.	14.6	80
60	Terahertz near-field microscopy of complementary planar metamaterials: Babinet's principle. Optics Express, 2011, 19, 2537.	3.4	88
61	Second harmonic generation based on strong field enhancement in nanostructured THz materials. Optics Express, 2011, 19, 7262.	3.4	38
62	Dispersion control with reflection grisms of an ultra-broadband spectrum approaching a full octave: erratum. Optics Express, 2011, 19, 12634.	3.4	0
63	Near-field investigation of induced transparency in similarly oriented double split-ring resonators. Optics Letters, 2011, 36, 1683.	3.3	19
64	Pulsed erbium fiber laser with an acetylene-filled photonic crystal fiber for saturable absorption. Optics Letters, 2011, 36, 3569.	3.3	7
65	THz Switching and THz Nonlinear Spectroscopy Applications. Chimia, 2011, 65, 316.	0.6	4
66	Spatiotemporal Visualization of THz Near-Fields in Metamaterial Arrays. Journal of Infrared, Millimeter, and Terahertz Waves, 2011, 32, 570-579.	2.2	4
67	Five picocoulomb electron bunch generation by ultrafast laser-induced field emission from metallic nano-tip arrays. Applied Physics Letters, 2011, 99, .	3.3	40
68	National Center of Competence in Research: molecular ultrafast science and technology. Chimia, 2011, 65, 292-3.	0.6	0
69	All-fiber frequency-stabilized erbium doped ring laser. Optics Express, 2010, 18, 26821.	3.4	12
70	Dispersion control with reflection grisms of an ultra-broadband spectrum approaching a full octave. Optics Express, 2010, 18, 27900.	3.4	37
71	Influence of finite spatial resolution on single- and double-pass femtosecond pulse shapers. Optics Letters, 2010, 35, 4072.	3.3	6
72	Radially polarized mode-locked Nd:YAG laser. Optics Letters, 2009, 34, 2030.	3.3	32

#	Article	IF	CITATIONS
73	Terahertz near-field imaging of electric and magnetic resonances of a planar metamaterial. Optics Express, 2009, 17, 3826.	3.4	123
74	Nanodoublers as deep imaging markers for multi-photon microscopy. Optics Express, 2009, 17, 15342.	3.4	71
75	Lattice modes mediate radiative coupling in metamaterial arrays. Optics Express, 2009, 17, 22108.	3.4	105
76	Optical Fibers With a Finite Metallic Core. Journal of Lightwave Technology, 2009, 27, 1454-1460.	4.6	2
77	Superbroadband fluorescence fiber fabricated with granulated oxides. Optics Letters, 2008, 33, 1050.	3.3	18
78	Understanding optimal control results by reducing the complexity. Chemical Physics, 2005, 318, 207-216.	1.9	21
79	Direct visualization of phonon-polariton focusing and amplitude enhancement. Journal of Chemical Physics, 2002, 117, 2897-2901.	3.0	14
80	Terahertz polariton propagation in patterned materials. Nature Materials, 2002, 1, 95-98.	27.5	95
81	Iterative Fourier transform algorithm for phase-only pulse shaping. Optics Express, 2001, 9, 191.	3.4	57
82	A MS-CASPT2 study of the low-lying electronic excited states of CH2BrCl. Chemical Physics Letters, 2001, 350, 155-164.	2.6	19
83	Application of nonreflecting boundary condition for numerical simulation of molecular photoionization dynamics. Journal of Applied Physics, 2000, 88, 2936-2942.	2.5	6